Communications: SIF Congress 2011

3D visualization of transplanted stem cells in infarcted rat hearts by high-resolution X-ray microtomography

A. Giuliani(*)

Dip.DISCO, Università Politecnica delle Marche - Via Brecce Bianche, Ancona, Italy
Consorzio Nazionale Interuniversitario per le Scienze fisiche della Materia - Ancona Unit
Via Brecce Bianche, Ancona, Italy
Istituto Nazionale Biostrutture e Biosistemi - Viale delle Medaglie d'Oro 305, Rome, Italy

Summary. — Stem-cell–based therapies involve the administration of *ex-vivo*–manipulated stem cell populations with the purpose of repairing and regenerating damaged tissues. To monitor the outcomes of stem cell therapy longitudinally requires the development of non-destructive strategies that are capable of identifying the location, magnitude, and duration of cellular survival and fate. In the field of cardiology the existence, in murine and human heart, of primitive cells able to generate all the different component structures of the myocardium has been recently documented. Synchrotron-Radiation–based X-Ray computed microtomography (SR-microCT) offers great potential to address these critical issues by non-invasively tracking the fate of the transplanted cells. In this review work, we explored the use of SR-microCT for detection of rat Cardiac Progenitor Cells, previously labeled with iron oxide tracers, inside the infarcted rat heart, one week after injection and in *ex vivo* conditions. This work on the one side strongly contributed to understand how and to which extent the injected cells are able to migrate and regenerate the damaged myocardium, on the other demonstrated that microCT appears to be an important way to investigate the cellular events involved in cardiac regeneration and represents a promising tool for future clinical applications.

PACS 87.57.nt – Edge enhancement.
PACS 87.57.Q- – Computed tomography.
PACS 87.59.-e – X-ray imaging.
PACS 87.85.Lf – Tissue engineering.

(*) E-mail: a.giuliani@univpm.it

1. – Introduction

Computed microtomography (microCT) and in particular Synchrotron-radiation–based computed microtomography (SR-microCT) have become in the recent years a useful tool for the structural analyses of different types of biomaterials and constructs in tissue engineering research. In fact, despite the fact that one of the first medical-related research fields in microCT was the analysis of trabecular bone samples [1], the use of this technique was quickly exploited to other areas of interest in life sciences including tissue engineering [2]. In particular this technique, allowing to analyse biomaterials (namely bioceramic and polimeric scaffolds) targeted for different applications in the life sciences, often requires approaches and settings that are completely different from each other.

Stem-cell–based tissue engineering therapies involve the administration of *ex-vivo–*manipulated stem cell populations with the purpose of repairing and regenerating damaged or diseased tissue. Currently available methods for monitoring transplanted cells are quite limited. To monitor the outcomes of stem cell therapy longitudinally requires the development of non-destructive strategies that are capable of identifying the location, magnitude, and duration of cellular survival and fate. Even in this case microCT and in particular SR-microCT offer great potentials to address these critical issues by non-invasively tracking the fate of the transplanted cells [3].

X-ray SR-microCT was successfully applied to investigate highly porous hydroxyapatite scaffolds [4], previously seeded with bone marrow stromal cells (BMSC), implanted in an immunodeficient murine model. It was proved that it was possible by using the microCT technique to obtain, in a non-destructive way, a quantitative analysis of tissue engineered constructs, determining the total volume and thickness distribution of newly formed bone into implants in a small animal model. Very recently, different ceramic scaffolds with high porosity were characterized [5] by using SR-microCT: the bone growth into the tissue engineered constructs was evaluated in *ex vivo* conditions and at different implantation times.

On the other side in the field of cardiology, clinical observations on the plasticity of adult stem cells have provided new tools for understanding the pathophysiology of cardiac diseases opening new strategies for the treatment of heart failure. Recent published reports [5-9] have contributed to identify the possible approaches of cellular therapy to generate new myocardium, involving systemic and local mobilization of progenitor cells. Moreover, different research groups [10-12] have recently documented the existence, in the adult murine and human heart, of primitive cells able to generate all the different component structures of the myocardium.

At the tissue level of organization, microscopy techniques attempting to visualize the tissue rebuilding process, such as light, fluorescence, scanning and transmission electron microscopy are limited to two-dimensional (2D) local information or, otherwise, require laborious three-dimensional (3D) reconstruction of serial sections.

A recent published report [13] comparing two 3D imaging methods—namely MRI and microCT—for *in vivo* preclinical studies on rodents, argued that both techniques require scan times that are much longer than a single respiratory or cardiac cycle. Real-time imaging is not possible with the current state of the art, unless active control of ventilation—that requires complex intubation of the animal—is performed. These serious limitations related to the observation of a beating heart, do not exist in the present work, which allows the visualization, in 3D and at high resolution (10–50 times higher than MRI), of the injected cells, with the possibility to quantify them and observe their fate within the myocardium one week after the injection.

In fact just recently, Torrente *et al.* [14] showed that X-ray microCT offers the possibility to visualize in 3D and in *ex vivo* conditions, with high definition and resolution, human CD133+ stem cells after transplantation and, therefore, opened new possibilities for experimental stem cell research

In the study reported in ref. [15] and for which here we propose a detailed review, we explored the use of microCT as an experimental technique with high spatial resolution for detection of rat Cardiac Progenitor Cells (rCPCs), previously labeled with iron oxide nanoparticles to increase the attenuation contrast, inside the infarcted rat heart, one week after injection and in *ex vivo* conditions. This work on the one side strongly contributed to understand how and to which extent the injected cells are able to migrate and regenerate the damaged myocardium, on the other demonstrated that SR-microCT offers the possibility of obtaining a 3D visualization of the cell spatial distribution and a quantification of the number of cells that are able to migrate from the site of injection to different areas of the rat heart tissue, with special reference to the infarcted myocardium.

2. – Materials and methods

2.1. *Sample preparation experimental protocol.* – The study population consisted of three male Wistar rats (*Rattus norvegicus*) breed in the animal facility of the University of Parma, Dept. of Pathology, age 12–14 wk, weighing 350–400 g. Myocardial infarction was produced in two rats by coronary binding of the left anterior descending coronary artery. Another sham-operated rat was treated similarly, except that the ligature around the coronary artery was not tied.

Cardiac Progenitor Cells (CPCs) were obtained from 3 month old Wistar rats by Langhendorff perfusion apparatus as described in [10] with minor modifications. Daily, microscopic observation of cultures showed the growth of two different adherent cell populations, one with mesenchymal-like and one with monomorphic blast-like characteristics. This latter population constituted the so-called Cardiac Progenitor Cells (CPCs) provided by clonogenic growth and multipotency [10].

To detect homing and engraftment of the injected cells into murine hearts, CPCs were loaded with iron oxide nanoparticles (Feridex–Poly-L-Lysine (PLL) complex composed of Fe 25 μg/ml + PLL 375 ng/ml) for 24 hours. Then, the medium was removed, CPCs washed with phosphate buffered saline (PBS) and trypsinized to be injected.

Three weeks after coronary ligature, a left lateral thoracotomy and mechanical ventilation was repeated in all animals under anaesthesia (Imalgene+Domitor). Two rats were treated with Feridex-labeled CPCs. Specifically, 5×10^5 CPCs suspended in 300 μl of IMDM+1% P/S supplemented with HGF (200 ng/ml) plus IGF-1 (200 ng/ml) were delivered in three regions bordering the scar. Each injection consisted of 100 μl. The third rat heart was injected with equal amounts of vehicle saline solution (PBS). Rhodamine microspheres, 2.0 μm in diameter (FluoSpheres, Molecular Probes, Eugene, USA), were added to each solution (5% of the total injected volume) to ensure the successful injection.

One week after the CPCs injection the animals were sacrificed.

The hearts of anesthetized animals were arrested in diastole by injection of 5 ml cadmium chloride solution (100 mmol, IV) and the myocardial vasculature shortly perfused at a physiological pressure with a heparinized PBS-solution, followed by perfusion with 10% formalin solution. The heart was then excised and placed in formalin solution (10%) for 24 hours.

After fixation, the rat hearts were completely dried immediately before their submission to microCT analysis.

The full investigation was approved by the Veterinary Animal Care and Use Committee of the University of Parma and conformed to the National Ethical Guidelines (Italian Ministry of Health; D.L.vo 116, January 27, 1992) and the Guide for the Care and Use of Laboratory Animals (NIH publication no. 85–23, revised 1996).

2$\cdot$2. *Synchrotron-radiation–based computed microtomography (SR-microCT).* – Attenuation based X-ray radiographic imaging is an invaluable standard tool, used routinely for non-destructive investigations in medicine [16,17]. However, the use of conventional attenuation-based X-ray microCT when investigating biological objects like hearts or cells, is often not appropriate because these tissues show only weak absorption contrast. On the other hand, the cross section for elastic scattering of X-rays in matter, which causes a phase shift of the wave passing through the object of interest, is usually much greater than that for absorption.

The in-line technique offers a very simple imaging set-up compared to other currently available X-ray phase-contrast imaging techniques. In fact in in-line, or propagation based, phase contrast imaging, phase contrast is achieved by simply letting the X-ray beam propagate in free space after interaction with the object. The contrast formation process can be understood in the framework of Fresnel diffraction [18].

When an X-ray beam passes through an object, it may be affected in two ways: it might be absorbed in the object, which changes its amplitude, and it might be retarded in the object, which changes its phase. For X-rays we can consider the object completely described by the complex refractive index $n = \varepsilon + \iota\beta$. Since ε is smaller than, but close to, unity for hard X-rays, the 3D complex refractive index distribution in the object can be written as

$$(1) \qquad\qquad n(x, y, z) = 1 - \delta_n(x, y, z) + i\beta(x, y, z),$$

where δ_n is the refractive index decrement, β is the attenuation index and (x, y, z) the spatial coordinates. Both quantities δ_n and β are real and positive. The amplitude and phase modulations introduced on the incident wave by the object can be described by a transmittance function [19]

$$(2) \qquad\qquad u_0(\mathbf{x}) = T(\mathbf{x})u_{\text{inc}}(\mathbf{x}),$$

where $u_{\text{inc}}(\mathbf{x})$ is the incident wave field, $u_0(\mathbf{x})$ the wave field at the exit plane of the object $(D = 0)$, $\mathbf{x} = (x, y)$ are the spatial coordinates in the plane perpendicular to the propagation direction z, and

$$(3) \qquad\qquad T(\mathbf{x}) = \exp[-B(\mathbf{x})]\exp[i\varphi(\mathbf{x})].$$

Both the attenuation and the phase shift induced by the object can be described as projections through the absorption and refractive index distributions respectively, with

$$(4) \qquad\qquad B(\mathbf{x}) = (2\pi/\lambda)\int \beta(x, y, z)\mathrm{d}z$$

and

$$(5) \qquad\qquad \varphi(\mathbf{x}) = -(2\pi/\lambda)\int \delta_n(x, y, z)\mathrm{d}z.$$

This means that both parts of the complex refractive index can be reconstructed by tomographic reconstruction if amplitude and phase can be measured for different angular settings of the sample. Phase contrast is achieved by simply recording the projections after a displacement of the detector away from the sample.

A microCT system available at the BM05 beamline of the European Synchrotron Radiation Facility (ESRF of Grenoble, France) was used in this work to non-destructively image and quantify the 3D microstructural morphology of the investigated rat hearts. The microCT experiment was performed with a 15 keV monochromatic X-ray beam and a sample-to-detector distance of 25 mm for the almost pure absorption-contrast and 500 mm for the phase-contrast, respectively. The acquisition set-up was based on previously described [14] 3D parallel tomography. 1500 projections and a step of 0.12 degrees were considered for each sample, with an exposure time of 1 s per projection.

3D reconstructions of the samples were obtained from the two series of 2D projections using a 3D filtered back projection algorithm implemented at ESRF. The different phases found in the histogram referring to the reconstruction of the in-absorption acquisition were segmented and rendered in colour using interactive software for the 3D imaging in order to make them more easily recognizable.

This data volume (absorption configuration) was then analysed in order to quantify the different phases by using the implementation of the 3D mean intercept length (MIL) method described in detail elsewhere [20, 21]. The different volumes were computed by counting the number of pixels labeled by the algorithm that automatically separates the different phases. The 3D MIL method was used, assuming a parallel-plate model, in order to derive the volume of the injected cells.

Volume rendering is a 3D visualization method by which the data volumes (absorption, phase contrast and combination of both) are rendered directly without decomposing it into geometric primitives. A Quad-Core Processor 2.01 GHz PC with 8 Gb RAM and the commercial software VGStudio MAX 1.2 were used to generate 3D images and to visualize in 3D the phase distribution. In order to achieve optimal settings for the image quality, we used Scatter HQ algorithm with an over sampling factor of 5.0 and activated color rendering. Being both the acquisitions performed simultaneously, the combining absorption and phase contrast images did not required their geometric warping so that the corresponding image is structured correctly. Therefore, synchronization may be interactive or partially or fully automatic with help of a fusion algorithm which is described elsewhere [22]. The full fusion automatic algorithm was used. This exact synchronization of data sets provides capacity for image fusion with superimposition of both sets of imaging data in one image data set for further 3D visualization.

3. – Results

The 3D distribution of rat CPCs, one week after their injection into an infarcted rat heart, was imaged and characterized by microCT both in absorption and in phase-contrast configuration. Two infarcted rat hearts, both injected with 5×10^5 Feridex®-labeled stem cells, were analyzed one week after CPCs injection. A third rat heart, not infarcted, injected only with the vehicle saline solution containing rhodamine particles was also investigated and considered as control.

The harvested heart samples were scanned and projection data were collected and processed to obtain a series of 2D images (stack of slices) of the hearts. Some representative reconstructed 2D slices, referred to an infarcted heart apex, are shown in fig. 1a and fig. 1b. The basic physical parameter quantified in each pixel of an absorption microCT
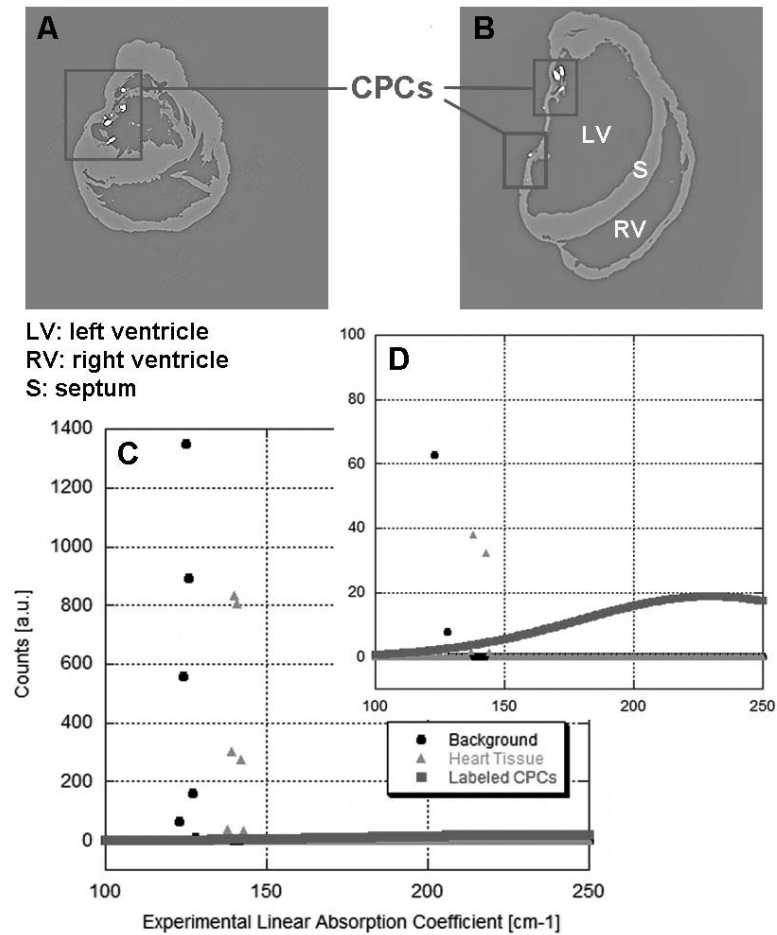
Fig. 1. – (A,B) Reconstructed 2D slices of a representative infarcted rat heart corresponding to axial sections at the level of the infarct. The infarcted area is well identifiable in the external wall of the left ventricle, where the wall is macroscopically thinner than the right ventricle and septum walls. The X-ray attenuation produced by the labeled CPCs is higher than attenuation referred to the other tissues, allowing their visualization as bright spots in the injured area. (C) The histogram of the grey level scale corresponding to the different detected phases [15]. (D) Magnification of the portion of the histogram shown in (C) referred to the peak corresponding to the labeled cells grey level [15].

slice is the linear X-ray attenuation coefficient μ. The X-ray attenuation produced by the Feridex-labeled transplanted CPCs is higher than attenuation produced by the myocardium of the injected hearts, allowing their visualization as bright spots in the 2D images (white spots in fig. 1a and fig. 1b). Different phases produce different X-Ray absorption rate within the samples that, in turn, translate into different peaks in the grey level scale. The histogram of the grey level scale is shown in fig. 1c and fig. 1d. The volume of each phase is obtained by multiplying the volume of a voxel (around $125\,\mu\mathrm{m}^3$) by the number of voxels underlying the peak associated with the specific phase. In the
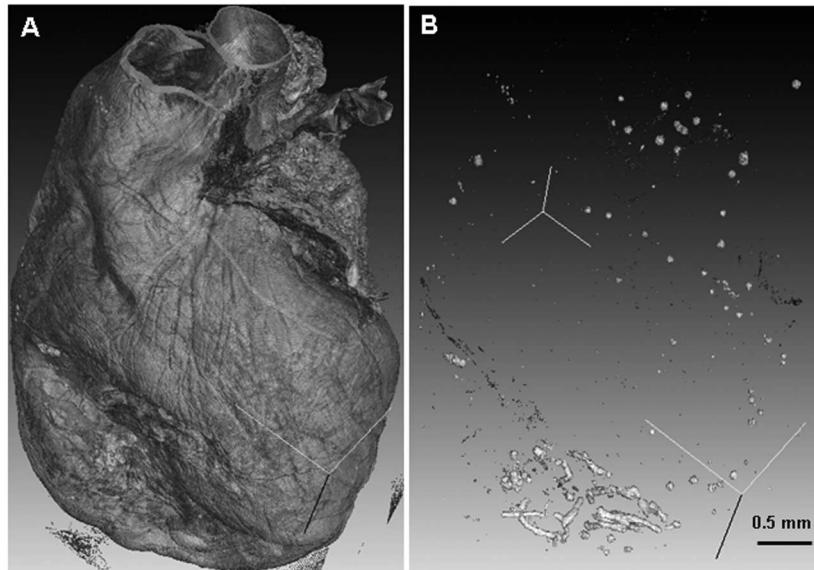
Fig. 2. – (A) 3D full reconstruction of a representative CPC-treated rat heart obtained by combination of absorbtion and phase-contrast signals (fusion method). (B) The segmentation process provides information on the distribution of labeled CPCs [15].

infarcted rat hearts, in agreement with the amount of the injected CPCs, their volume percentage with respect to the total investigated volume is very low. This fact explains why the peak corresponding to the labeled CPCs cannot be revealed in fig. 1c but, magnifying the respective portion of the histogram, it can be easily visualized in fig. 1d.

The slices were compiled in a stack to render 3D reconstructions of the investigated rat hearts with the aim to obtain a realistic volumetric visualization of the stem cell distribution after their injection in the infarcted rat hearts.

3D images obtained combining absorption and phase-contrast signal using the fusion technique are represented in fig. 2. In combined imaging, morphological information about heart tissue from phase contrast (fig. 2a) is complemented and extended by the functional information on labeled-CPCs supplied from absorption mode. In fact, the simple segmentation of the histogram referred to the set of data produced with the absorption set up provides information on the internal structure of the heart and the distribution of the CPCs within it (fig. 2b). In particular in fig. 2 all the phases of the rat heart were represented. Processing the 3D image of the heart it is also possible to make one or more phases translucent or even to "cancel" a phase in order to allow a more accurate observation of the spatial distribution of each phase. In fig. 2b we virtually deleted the heart tissue phase for a better visualization of the labeled CPCs in the different areas of the rat heart.

No dramatic difference in the location of stem cells was observed in the two infarcted hearts: the percentage of migrated labeled stem cells from the injection area to the infarcted area or towards other areas was calculated by counting their corresponding pixels, using the algorithm that automatically separates them from the other tissues [15]. No detectable spots were found in the rat heart injected with only the vehicle saline solution containing rhodamine particles, demonstrating that the bright spots in the cell-treated infarcted hearts correspond to labeled CPCs. Portions of the 3D reconstruction referred
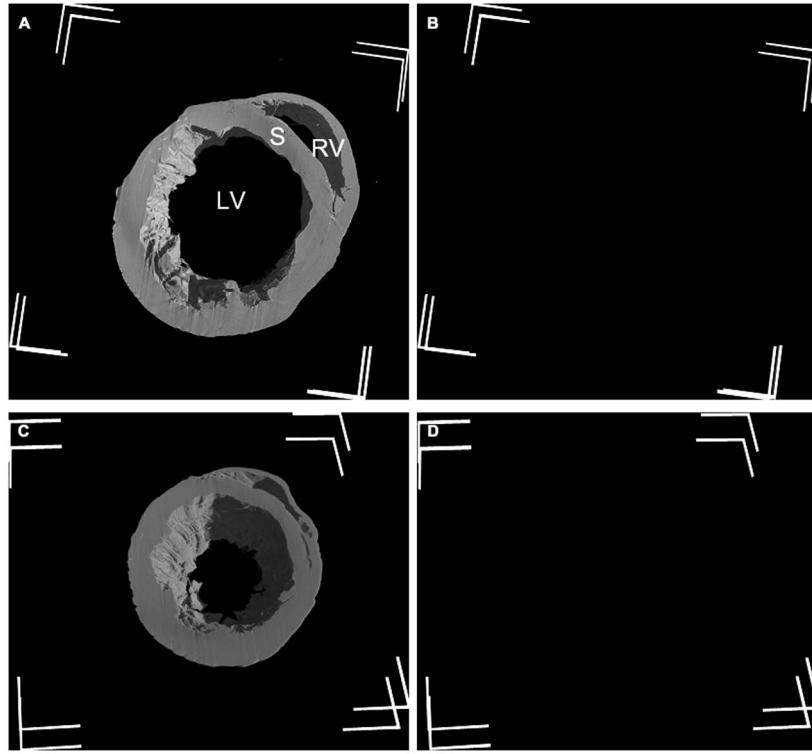
Fig. 3. – MicroCT 3D reconstructions of the not-infarcted heart injected with only the vehicle saline solution containing rhodamine particles. LV: left ventricle; RV: right ventricle; S: septum. (A, C) Two 3D portions of the bottom part of the heart corresponding to the apex largely involved by infarction in the other infarcted hearts. (B,D) Same volumes as in (A) and (C), respectively—all the phases were virtually made transparent beside the portion of the histogram corresponding to the labeled cells in the infarcted hearts. No cells are visible both in the right and left ventricle.

to the control rat heart (lower part corresponding to the infarcted area in the two CPC-treated hearts) are represented in fig. 3. Figure 3b and fig. 3d demonstrate that, after the same 3D image processing (segmentation) used for the infarcted hearts, no bright signals can be found in this control sample.

4. – Discussion

The main interest in combining phase imaging to attenuation-based microCT is the improved sensitivity the former offers compared to the latter. The gain in sensitivity in the hard–X-ray range can be several orders of magnitude for soft materials, which makes it appealing for biomedical imaging of soft tissues, including studies of adult autologous cellular therapy for the treatment of acute and chronic myocardial infarction. On the other hand, many unresolved questions limit at the moment the challenge to link experimental with clinical observations, concerning the fate of transplanted stem cells in the recipient tissue and the specific tracing of engrafted cells or cell populations detectable by imaging techniques.

Fig. 4. – 3D image of the infarcted area obtained with the fusion method [15]. Two different structures have been individuated: a rounded-shape one, typical for the CPCs also in the original *in vitro* cultures, and the other made of oriented rod-shaped structures, most likely cells grouped in finger-like clusters.

In ref. [15] the microCT was used to image and characterize the 3D spatial distribution of injected rat clonogenic cells (CPCs) after their labeling by iron oxide nanoparticles, inside the heart tissue of infarcted rats. The 3D visualization of the spatial distribution of the injected CPCs with respect to myocardium was obtained. In particular, being the X-ray attenuation produced by the labeled cells higher than that of host myocardial tissues, we achieved their visualization as bright spots both in the 2D slices (fig. 1a and fig. 1b) and in the whole 3D reconstructions (fig. 2). One week after injection, labeled cells were distributed mostly in proximity and towards the damaged infarcted area (fig. 2b), demonstrating migration of CPCs from the injection site towards the injured myocardium. Structures with two different morphologies were detected: one rounded-shaped, typical for the CPCs also in the original *in vitro* cultures, and the other made of oriented rod-shaped structures, likely cells grouped in finger-like clusters (fig. 4). This is a very useful piece of information not detectable by conventional histological methods. We also observed single cell units in all areas of the heart, as in the atria, in large vessels and in the right ventricle (fig. 2b), confirming that the injected CPCs can migrate through the myocardium by biological mechanisms that are still not fully understood.

The fact that no X-ray absorption contrast was found within the rat heart injected with only saline solution and rhodamine particles suggests that microCT is able to detect at 3D level and at high resolution the migrating labeled cells.

Furthermore these microCT results are in close agreement with the imaging of the distribution of QDots-labeled CPCs injected in identically treated infarcted rat hearts [15]. Also this fact suggests the validity of the microCT to detect cell migration and engraftment within the injured heart.

On the other hand, the issue whether either iron particles, as detected here by MicroCT, or QDots nanoparticles, as detected by UV excitation, could only represent unreliable signals of macrophages uptaking tracers released by dying cells, remains an unresolved problem especially on clinical ground. Because of that, in ref. [15] a third independent genetic marker was applied to visualize the progeny of the injected cells. This approach allowed us to ensure that the progeny of the injected cells was present in the infarcted heart and with a similar distribution to that observed with QDots labeling and MicroCT imaging. Importantly, by this third genetic-marker–based approach, the differentiation of CPCs into cardiomyocytes was also demonstrated. This induced the authors of ref. [15] to estimate, by quantitative analysis of the microCT data, the total number N of the cells found in the hearts one week after CPC injection.

By this quantitative analysis, they found out that in both the infarcted hearts the number N of CPC-derived cells is more than doubled with respect to the number of injected CPCs, demonstrating that, at least for labeled CPCs and at a week from injection, the presence of iron oxide nanoparticles does not dramatically affect the CPC fate.

However it has to be stressed that, before the introduction of the available imaging methodologies, including microCT, in the clinical practise, it is necessary to clarify several issues. For instance, at which extent the microCT in absorption configuration is able to detect the injected cells even after their proliferation with the consequent hyperdilution (possibly below the detection limit) of the iron oxide tracer on dividing cells.

Further follow-up studies are required to explore the potentialities in this field of the in-line, or propagation-based, phase contrast imaging. In fact, the main interest in phase imaging is the improved sensitivity it offers compared to attenuation-based techniques [18]. The gain in sensitivity in the hard–X-ray range can be several orders of magnitude for soft materials, even in the absence of any tracer, which makes it appealing for biomedical imaging of soft tissues, including stem-cell–treated infarcted hearts. The possibility to perform in-line microCT investigation in soft tissues, without the need of any contrast agent, would provide new insights not only in the imaging of soft tissues and cells but also, in cardiology, would achieve the possibility to study remote time points after cell injection, definitively avoiding the possibility that bright spots in 3D microCT images represent macrophages that have phagocytized iron nanoparticles, or highly absorbent particles that have been expelled from injected cells into the interstitium.

In conclusion, the 3D images produced in ref. [15] represent a very innovative progress, as compared to the usual 2D histological images, which do not provide the overall 3D distribution of the injected stem cells within the heart. Furthermore, these observations strongly support further studies aiming to support the contention that phase contrast microCT represents a new 3D-imaging way to investigate the cellular events involved in cardiac regeneration and represents a promising tool for other applications in regenerative medicine.

* * *

REFERENCES

[1] Feldkamp L. A., Goldstein S. A., Parfitt A. M. Jesion G. and Kleerekope M., *J. Bone Min. Res.*, **4** (1989) 3.

[2] Ho S. T. and Hutmacher D. W., *Biomaterials*, **27** (2006) 1362.

[3] Belicchi M., Cancedda R., Cedola A., Fiori F., Gavina M., Giuliani A., Komlev V. S., Lagomarsino S., Mastrogiacomo M., Renghini C. Rustichelli F., Sykovà E. and Torrente Y., *Mater. Sci. Eng. B*, **165** (2009) 139.

[4] Komlev V. S., Peyrin F., Mastrogiacomo M., Cedola A., Papadimitropoulos A., Rustichelli F. and Cancedda R., *Tissue Eng.*, **12** (2006) 3449.

[5] Komlev V., Mastrogiacomo M., Pereira R. C., Peyrin F., Rustichelli F. and Cancedda R., *Eur. Cells Mater.*, **19** (2010) 136.

[6] Kajstura J., Rota M., Whang B., Cascapera S., Hosoda T., Bearzi C. *et al.*, *Circ Res.*, **96** (2005) 127.

[7] Kajstura J., Urbanek K., Rota M., Bearzi C., Hosoda T., Bolli R., Anversa P. and Leri A., *J. Mol. Cell Cardiol.*, **45** (2008) 505.

[8] Wollert K. C., Meyer G. P., Lotz J., Ringes-Lichtenberg S., Lippolt P., Breidenbach C. *et al.*, *Lancet*, **364** (2004) 141.

[9] Balsam L. B., Wagers A. J., Christensen J. L., Kofidis T., Weissman I. L. and Robbins R. C., *Nature*, **428** (2004) 668.

[10] Beltrami A. P., Barlucchi L., Torella D., Baker M., Limana F., Chimenti S. *et al.*, *Cell*, **114** (2003) 763.

[11] Oyama T., Nagai T., Wada H., Naito A. T., Matsuura K., Iwanaga K. *et al.*, *J. Cell Biol.*, **176** (2007) 329.

[12] Barile L., Chimenti I., Gaetani R., Forte E., Miraldi F., Frati G. *et al.*, *Nat. Clin. Pract. Cardiovasc. Med.*, **4** (2007) S9.

[13] Badea C. T., Bucholz E., Hedlund L. W., Rockman H. A. and Johnson G. A., *Toxicologic Pathology*, **34** (2006) 111.

[14] Torrente Y., Gavina M., Belicchi M., Fiori F., Komlev V., Bresolin N. *et al.*, *Febs Lett.*, **580** (2006) 5759.

[15] Giuliani A., Frati C., Rossini A., Komlev V. S., Lagrasta C., Savi M., Cavalli S., Gaetano C., Quaini F., Manescu A. and Rustichelli F., *J. Tissue Eng. Regen. Med.* (2011). DOI: 10.1002/term

[16] Hajnal J. V., Hill D. L. G. and Hawkes D. J. (Editors), *Medical Image Registration* (CRC Press, Boca Raton) 2001.

[17] Baert A. (Editor), 2008; *Encyclopedia of Diagnostic Imaging* (Springer: Berlin) 1965, pp. 1334.

[18] Langer M., Boistel R., Pagot E., Cloetens P. and Peyrin F., in *Microscopy: Science, Technology, Applications and Education*, edited by Méndez-Vilas A. and Díaz J. (Formatex, Spain) 2010, pp. 391-402.

[19] Goodman J. W., *Introduction to Fourier Optics*, 3rd edition, (Greenwood Village, CO, Roberts & Co.) 2005.

[20] Salome M., Peyrin F., Cloetens P., Odet C., Laval-Jeantet A. M., Baruchel J. *et al.*, *Med. Phys.*, **26** (1999) 2194.

[21] Peyrin F., Salome M., Cloetens P., Laval-Jeantet A. M., Ritman E., Rüegsegger P. *et al.*, *Health Care*, **6** (1998) 391.

[22] Stokking R., Zubal I. G. and Viergever M. A., *Semin. Nucl. Med.*, **33** (2003) 219.